Clim. Past Discuss., https://doi.org/10.5194/cp-2018-141
Manuscript under review for journal Clim. Past
Discussion started: 29 October 2018

Climate of the Past Discussions
Open Access
EGU

Warm-season hydroclimate variability in Central China since 1866 AD and its relations with the East Asian Summer Monsoon: evidence from tree-ring earlywood width

Yesi Zhao[1,2], Jiangfeng Shi[1,3], Shiyuan Shi[1], Xiaoqi Ma[1], Weijie Zhang[1], Bowen Wang[1], Xuguang Sun[4], Huayu Lu[1], Achim Bräuning[2]

[1] School of Geography and Ocean Science, Nanjing University, Nanjing 210023, China
[2] Institute of Geography, Friedrich-Alexander-University Erlangen-Nürnberg, Erlangen 91058, Germany
[3] Laboratory of Tree-Ring Research, University of Arizona, Tucson 85721, USA
[4] School of Atmospheric Sciences, Nanjing University, Nanjing 210023, China

Correspondence to: Jiangfeng Shi (shijf@nju.edu.cn)

Abstract. Historical hydroclimate records derived from tree-ring parameters are scarce in the core region of East Asian Summer Monsoon (EASM) in China, limiting our understanding of the inter-decadal hydroclimate variability of this region and its possible connections with the EASM. In this study, standard chronologies of total tree-ring width (TRW), earlywood width (EWW), and latewood width (LWW) were created using tree-ring samples of *Pinus tabulaeformis* in the eastern Qinling Mountains, Central China. The strongest growth-climate relationship was found between EWW and May–July self-calibrated Palmer Drought Severity Index (MJJ scPDSI). Therefore, a linear regression model, which explained 50.3% of the variance in MJJ scPDSI (1951–2005), was developed to estimate the past MJJ scPDSI variations using EWW. The time series of MJJ scPDSI was extended back to the year 1866, and validated by independent hydroclimate series from nearby regions. Before the mid-1950s, the variations of MJJ scPDSI were in-phase with those of EASM intensity on decadal and longer timescales, suggesting that wet conditions would occur in the eastern Qinling Mountains when EASM was strengthened. Since the mid-1950s, however, the relationship has been out-of-phase. This phase change may be associated with an intensified dipole pattern of EASM precipitation.

1. Introduction

Anomalous East Asian Summer Monsoon (EASM) activity can cause severe drought and flood events in its impact area, leading to great loss of lives and property (Ding, 1992; Huang et al., 2006). Interdecadal variability of EASM and the related hydroclimatic changes have been topics intensively discussed in China's climate research community (Zhou et al., 2017). Since quality-controlled instrumental records started in the 1950s in China (Zhou et al., 2009), most studies only focused on the past 60 years when exploring the EASM-hydroclimate relationship. Nevertheless, Wang et al. (2000) developed a precipitation dataset which extended back to 1880, enabling it possible to study the relationship between EASM and hydroclimate before the 20th century (Ding et al., 2008; Guo et al., 2004; Zhou et al., 2009). However, the reliable period of

Clim. Past Discuss., https://doi.org/10.5194/cp-2018-141
Manuscript under review for journal Clim. Past
Discussion started: 29 October 2018

this dataset only began in the early-stage of 20th century (Zhou et al., 2009). Therefore, to study the long-term relationship between EASM and hydroclimate, reconstructions using climate proxies such as tree rings, ice cores, or historical documents are needed (Ding et al., 2013).

Tree-rings have significant advantages over other proxies in some important aspects, including annual resolution, replication, and preservation of high-frequency signals (Meko and Graybill, 1995). Therefore, they are an ideal source for studying climatic variations on inter-annual to multi-decadal timescales. Previous tree-ring studies relevant to EASM variability were mainly concentrated in arid and semi-arid regions that belong to the marginal areas of EASM influence (Chen et al., 2013; Liang et al., 2007; Liu et al., 2017b; Yang et al., 2013a). However, the impacts of EASM on hydroclimate variability vary spatially (Guo et al., 2004; Zhou et al., 2009). In the core monsoon region of China, a predominant feature of EASM is the Mei-yu rainfall, which has a nearly east-west distribution pattern in the region 27°–35°N, 105°–125°E during mid-June to mid-July. The summer rainfall over the Mei-yu region has been considered as a good representation of EASM variability (Wang et al., 2008). Therefore, hydroclimate reconstructions within the representative region of EASM are necessary. Numerous studies have indicated that tree-ring width mainly reflects temperature signals in the humid and semi-humid EASM core region (Cai and Liu, 2016; Duan et al., 2012; Shi et al., 2017; Shi et al., 2010; Zheng et al., 2012), and suggested the use of tree-ring stable isotopes to capture hydroclimate signals (Cai et al., 2018; Liu et al., 2017a; Xu et al., 2016; Xu et al., 2018). However, robust hydroclimate signals can also be extracted from tree-ring width at some low-altitude and well-drained sites as evidenced by several recent studies (Cai et al., 2017; Chen et al., 2016a; Shi et al., 2015). Furthermore, studies indicate that using tree-ring parameters with sub-annual resolution, such as earlywood width (EWW) and latewood width (LWW), might be a way to obtain stronger hydroclimate signals than using total tree-ring width (TRW) (Chen et al., 2012; Zhao et al., 2017a; Zhao et al., 2017b). These findings inspired us reconstructing hydroclimate variations using sub-annual tree-ring width in the core EASM region.

The eastern Qinling Mountains are located in the central EASM region, and are characterized by a transitional climate from warm-temperate to subtropical. In this region, only a few tree-ring based hydroclimate reconstructions have been conducted in Mount Hua (Chen et al., 2016b; Hughes et al., 1994; Liu et al., 2002), and Mount Yao (Liu et al., 2017a). Shi et al. (2012) studied the climate-growth relationships of *Pinus tabulaeformis* along an elevation gradient in Mount Funiu. All sampling sites in Shi et al. (2012) were located on mountain tops, where soils are thin and well-drained. The TRW chronologies at the two low-altitude sites, Baiyunshan (BYS) and Longchiman (LCM), exhibited a weak response to summer hydroclimate variability. Due to increased temporal resolution of intra-annually resolved tree-ring records, we hypothesize that hydroclimate signals contained in EWW or LWW are stronger than those in whole TRW. Therefore, our aims in the present study are determined to: (1) compare the climate sensitivity of tree-ring EWW, LWW, and TRW in *P. tabulaeformis* at BYS and LCM; (2) attempt to reconstruct regional hydroclimate variability using the parameter that contains the strongest hydroclimate signals; (3) explore the relationship between the reconstructed hydroclimate variability and EASM.

Clim. Past Discuss., https://doi.org/10.5194/cp-2018-141
Manuscript under review for journal Clim. Past
Discussion started: 29 October 2018

2. Materials and Methods

2.1. Study sites and tree-ring data

Dated tree-ring samples of *P. tabulaeformis* used in this study were provided by Shi et al. (2012). They were collected from two sampling sites in Mount Funiu in 2006 and 2008: BYS (33.63° N, 111.85° E) and LCM (33.68° N, 112.05° E) (Fig. 1). The elevations of BYS and LCM range from 1200–1300 m above sea level (asl), and 1340–1400 m asl, respectively. Although there are some differences in elevation, the TRW chronologies of these two sites were significantly correlated ($r = 0.75$, $p < 0.01$) from 1887 to 2005, and share a similar climate-growth relationship (Shi et al., 2012). The regional annual mean temperature and annual total precipitation are 13.9°C and 752 mm, respectively. A major part of the annual precipitation is recorded during the warm season (Fig. 2). More detailed information on the study sites can be found in Shi et al. (2012).

P. tabulaeformis generally exhibits an abrupt transition from light-colored earlywood to dark-colored latewood (Liang and Eckstein, 2006; Fig. 3). Due to this wood anatomical characteristic, the earlywood and latewood segments of annual growth rings can be confidentially discriminated visually by the sudden change in cell size, lumen size, and color (Stahle et al., 2009). However, gradual transitions also occurred in a few samples, making the exact delineation of the earlywood-latewood boundary difficult. Therefore, only samples with distinct earlywood and latewood segments were used for subsequent measurements (Knapp et al., 2016). In total, 20 cores from 11 trees and 42 cores from 22 trees were selected from BYS and LCM, respectively. EWW and LWW were then measured using a LINTAB5 system at a resolution of 0.001 mm, and TRW was obtained by adding EWW and LWW together.

Standardized EWW, LWW, and TRW chronologies were developed using the ARSTAN program (Cook, 1985). Firstly, the age-dependent growth trends in the measurement series were fitted by negative exponential or linear regression curves, and two series at LCM01 with anomalous growth trends were fitted by cubic splines with a 50% frequency-response cutoff equal to 67% of the series length. Secondly, all width index series were calculated as ratios of original ring widths and the fitted trends, and merged into a regional standard chronology using the bi-weight robust mean method. Lastly, to minimize the effects of sampling depth changes, the variance of each chronology was stabilized according to the method described by Osborn et al. (1997). EPS (expressed population signal) and Rbar were calculated over 30-year windows with a 15-year overlap were used to evaluate the quality of the width chronologies (Cook et al., 1999; Wigley et al., 1984). Rbar represents the mean of all correlations for tree-ring width index series between each pair of cores. EPS is a function of Rbar and sample size, and is used to estimate how well the sample chronology represents the theoretical chronology.

2.2. Climatic data and statistical methods

To investigate the climate-growth relationship, monthly mean temperature and monthly total precipitation were selected from nearby meteorological stations (Luanchuan: 33.78° N, 111.6° E, 750.3 m asl; Xixia: 33.3° N, 111.5° E, 250.3 m asl; Lushi: 34.05° N, 111.03° E, 568.8 m asl; Sanmenxia: 34.8° N, 111.2° E, 409.9 m asl; Laohekou: 32.38° N, 111.67° E, 90 m asl; Fig. 1b). These climate data were obtained from the China Meteorological Data Service Center (CMDC), and were quality checked

before release. Regional temperature values were calculated by averaging the station temperature time series. Regional precipitation values were produced by firstly averaging the standardized anomalies of station precipitation time series, then transforming the averaged standardized anomalies back to the original unit of precipitation (Jones and Hulme, 1996). Regional hydroclimate conditions were represented by the monthly self-calibrating Palmer Drought Severity Index (scPDSI) averaged in the area between 32° N to 35° N and 110° E to 112° E, which were extracted from the global land scPDSI dataset (van der Schrier et al., 2013). The scPDSI reflects soil moisture availability, and has been proved to be a good proxy for studying wet and dry spells across China (Li et al., 2009; Wang et al., 2017). Pearson's correlation coefficients (r) were calculated to explore the climate-growth relationship from previous July to current December over the period 1951–2005. In addition, partial correlation and moving correlation analyses were performed to evaluate the robustness of the relationships between radial growth and its limiting climatic factors. The significance of correlation coefficients was tested using two-tailed t-statistic.

For hydroclimate reconstruction, a simple linear regression model was applied to establish a transfer function. Temporal stability of the model was tested by a split calibration-verification procedure using the following statistics: r, explained variance (R^2), reduction of error (RE), coefficient of efficiency (CE), and the sign-test (Meko and Graybill, 1995). Spatial correlations of the reconstructed series were analysed using the KNMI Climate Explorer (http://climexp.knmi.nl/start.cgi). In order to validate our hydroclimate reconstruction, it was compared with several hydroclimate reconstructions and historical document records, including (1) the scPDSI time series averaged from the subset (32° N–35° N, 110° E–112° E) of the scPDSI dataset for global land (van der Schrier et al., 2013), (2) the June–August PDSI from the No. 370 grid point of the Monsoon Asia Drought Atlas (MADA) at 32.75° N, 113.75° E (Cook et al., 2010), (3) the dryness/wetness index (DWI) from the grid point at 32.75° N, 113.75° E (Yang et al., 2013b), (4) reconstructed April–June precipitation based on TRW in Mount Hua (Chen et al., 2016b), and (5) drought/wet events recorded in historical documents (Wen, 2006).

Several EASM indices (EASMI) with different notions have been proposed to measure EASM strength. Wang et al. (2008) suggested that an appropriate EASMI should be able to reflect the principal mode of EASM rainfall variability, and highlight the significance of Mei-yu rainfall in gauging EASM strength. Following this suggestion, Zhao et al., (2015) defined a new EASMI based on 200 hPa zonal wind anomalies, which captures the dominant modes of rainfall variability over East Asia. We calculated the May–July (MJJ) EASMI according to the definition of Zhao et al. (2015). The used 200 hPa zonal wind dataset was obtained from the National Oceanic and Atmospheric Administration-Cooperative Institute for Research in Environmental Sciences (NOAA/CIRES) Twentieth Century Reanalysis V2c (NOAA-20C; Compo et al., 2011). We selected this dataset because it covers the period 1851 to 2014, and hence is the longest currently available dataset at present. Further, the MJJ EASMI calculated using this dataset is highly consistent with another EASMI (Zhao et al., 2015) calculated from the Japanese 55-year Reanalysis Project dataset (JRA-55; Kobayashi et al. 2015; Fig. 5). The relationship between MJJ EASMI and our reconstruction was evaluated using Pearson's correlation analyses. To highlight decadal and longer climate fluctuations, MJJ EASMI and our reconstruction were filtered using a low-pass Fast Fourier Transform (FFT) with a cutoff frequency of 0.1 Hz. The significance was adjusted for the correlations between the two decadal filtered time series because their degrees of freedom had reduced to one fifth of the initial (Yan et al., 2003). In addition, to understand the impacts of EASM on

Clim. Past Discuss., https://doi.org/10.5194/cp-2018-141
Manuscript under review for journal Clim. Past
Discussion started: 29 October 2018

hydroclimate variability on a spatial perspective, spatial correlation analyses were performed with the gridded precipitation dataset from Global Precipitation Climatology Centre Version 7 (GPCC v7; Schneider et al., 2015), and gridded temperature dataset from Climatic Research Unit Time-Series Version 4.01 (CRU TS 4.01; Harris et al., 2014). These gridded datasets are capable of reproducing precipitation and temperature variability over East China during the 20th century (Wang and Wang, 2017; Wen et al., 2006).

3. Results and Discussion

3.1. Chronology characteristics

The established chronologies and corresponding EPS, Rbar, and sample size values are shown in Fig. 4. Each of the chronologies had a total length of 165 years, spanning from 1841 to 2005. During the whole period, the EWW chronology generally exhibited higher EPS and Rbar values than the LWW chronology, indicating that stronger common signals were shared by earlywood growth than latewood growth. Similar EPS and Rbar values were found between the TRW and EWW chronologies, which could be attributed to the fact that EWW represents the majority of TRW (on average, the portion of EWW of TRW accounts for 65.8%). According to the generally accepted EPS threshold value of 0.85 (Wigley et al., 1984), the reliable period of EWW and TRW chronologies was 1866–2005, and 1881–2005 for the LWW chronology, respectively.

3.2. Climate-growth relationship

As shown in Fig. 6, EWW is significantly positively correlated with precipitation in May, but negatively correlated with temperature in May–June. These results highlight the effect of drought stress during the main growing season. EWW is more sensitive to scPDSI, with the highest correlation ($r = 0.71$, $p < 0.01$) being found in MJJ. When the effects of temperature and precipitation signals are removed by partial correlation, EWW still has a high correlation ($r = 0.59$, $p < 0.01$) with MJJ scPDSI. In addition, the linear relationship between EWW and MJJ scPDSI is more time stable than those between EWW and MJJ temperature or precipitation (Fig. 7). All these results indicate that earlywood growth is primarily controlled by MJJ scPDSI. By contrast, LWW almost has no significant correlations with precipitation and temperature. Meanwhile, LWW showed a much lower positive correlation with MJJ scPDSI (Fig. 6). This indicates that latewood growth is less sensitive to climate than earlywood. The low climate sensitivity of LWW also induces a weaker climate-growth relationship for TRW than for EWW (Fig. 6).

The highest correlation coefficient between EWW and MJJ scPDSI suggests that MJJ moisture availability is the dominant environmental factor limiting radial growth of *P. tabulaeformis* in LCM and BYS. Fast radial growth of *P. tabulaeformis* usually happens in the early growing season (Liang et al., 2009; Shi et al., 2008; Zeng et al., 2018). Increased water deficiency in the early growing season could suppress cell expansion and cell growth in the cambium (Fritts, 1976), resulting in the formation of narrow rings. Such climate-growth relationships of *P. tabulaeformis* are consistent with findings from previous

Clim. Past Discuss., https://doi.org/10.5194/cp-2018-141
Manuscript under review for journal Clim. Past
Discussion started: 29 October 2018

studies (e.g. Cai and Liu, 2012; Cai et al., 2014; Cai et al., 2015; Chen et al., 2014; Fang et al., 2009; Fang et al., 2012b; Li et al., 2006; Liang et al., 2006; Liu et al., 2017b; Shi et al., 2008; Song and Liu, 2011; Sun et al., 2012).

3.3. Hydroclimate reconstruction and comparison

Based on the above analyses, we selected MJJ scPDSI as the target for hydroclimate reconstruction. The EWW chronology was chosen as the predictor (Fig. 8a). The transfer function between EWW chronology and MJJ scPDSI was estimated using a simple linear regression model as expressed in Eq. (1):

$$\text{MJJ scPDSI} = 4.45\text{EWW} - 4.06; (R^2 = 0.503, n = 55, p < 0.001)\ , \quad (1)$$

The model explains 50.3% of the actual MJJ scPDSI variance over the period of 1951–2005. The calibration-verification tests show that r, R^2 and the sign-test are significant at the 0.01 level, and that *RE* and *CE* values are positive (Table 1). In addition, the first-order differences of MJJ scPDSI and EWW are strongly linearly correlated (Fig. 8b). All test results confirm that the model is valid (Cook et al., 1999; Fritts, 1976).

Based on the above model, the MJJ scPDSI of the study region was reconstructed back to 1866 (Fig. 8c). We restored the variance of reconstruction to match the variance of instrumental MJJ scPDSI during the calibration period. Spatial correlation analysis indicates that the reconstruction most strongly represents Central China, including the western part of Henan, the northern part of Hubei, and the southern part of Shaanxi provinces (Fig. 1a). Our reconstruction is significantly correlated with the instrumental scPDSI series (r = 0.47; p < 0.01; 1901–2005) (Fig. 9a), and the PDSI series of MADA 370 (r = 0.43; p < 0.01; 1866–2005) (Fig. 9b). However, the unprecedented drying trend that began in the early 1990s in MADA was not found both in our reconstruction and the instrumental scPDSI series, implying that MADA may have overestimated drought severity over the past two decades in the study area. This overestimation was also found in the Guancen Mountains, North China (38.83° N, 112.08° E). We assume that this discrepancy was probably due to the insufficient spatiotemporal distribution of the tree-ring network used in MADA, and many of the tree-ring data used ended in the 1990s (Li et al., 2015). Our reconstruction is also significantly correlated with the nearby DWI (r = –0.22; p < 0.05; 1866–2000) (Fig. 9c), and a tree-ring based precipitation reconstruction for southeast China (r = 0.49; p < 0.01; 1866–2005) (Fig. 9d). Moderately to severely dry (wet) events are normally defined by scPDSI values less than –2 (larger than 2), if the scPDSI time series has a mean of zero (Palmer, 1965). Since the reconstructed MJJ scPDSI fluctuates around the mean of 0.29, we define moderately to severely dry (wet) events as MJJ scPDSI values below -1.71 (above 2.29). Based on these criteria, 10 anomalously dry years and 11 anomalously wet years were identified during the period 1866–1950. Most of the anomalously dry (wet) years could be verified by corresponding descriptions in historical documents (Fig. 9e; Table 2). The low-frequency variation shows that common drought periods occurred in the 1870s and 1920s. These drought periods were also observed in North and West China (Cai et al., 2014; Chen et al., 2014; Fang et al., 2012a; Kang et al., 2013; Liang et al., 2006; Liu et al., 2017b; Zhang et al., 2017), indicating that these droughts had widespread impacts. The above comparisons suggest that our reconstruction is able to capture the broad-scale warm-season hydroclimate variability in this region.

Clim. Past Discuss., https://doi.org/10.5194/cp-2018-141
Manuscript under review for journal Clim. Past
Discussion started: 29 October 2018

3.4 Connections with EASMI

A significant positive correlation ($r = 0.23$, $p < 0.01$) exists between MJJ scPDSI and EASMI during the period 1866–2005. The correlation coefficient becomes 0.43 ($p < 0.05$) after a 10-year low-pass filter was applied for the two time series, suggesting that MJJ scPDSI and EASMI are generally in-phase on the decadal and longer timescales. However, a careful check revealed that the in-phase relationship was unstable: the two series are in-phase ($r = 0.62$, $p < 0.01$) during 1866–1956, but out-of-phase ($r = –0.29$) during 1957–2005 (Fig. 10). The relationship changed around the mid-1950s.

Spatial correlation analyses showed positive correlations between the decadal filtered MJJ EASMI and scPDSI in the Yellow-Huaihe River basins during 1901–1956, but negative correlations during 1957–2005 (Fig. 11a–b). In terms of precipitation, positive correlations are found over the Yangtze-Huaihe-Yellow River basins during 1901–1956 (Fig. 11c). From 1957 to 2005, positive correlations retreat southward to the Yangtze River basin and South China, with negative correlations emerging in the Yellow-Huaihe River basins, manifesting a dipole pattern of EASM precipitation (Fig. 11d). Pei et al. (2015) also suggested that a dipole pattern had intensified since the 1950s, which might be associated with the forcings of the Atlantic Multi-decadal Oscillation (Si and Ding 2016). On the contrary, temperature has much weaker correlations with EASMI over the Yellow-Huaihe River basins, and there are no significant spatial pattern changes (Fig. 11e–f). Therefore, it is precipitation that plays a dominant role in altering the correlation pattern between MJJ scPDSI and EASMI on decadal and longer timescales.

4. Conclusions

A new tree-ring based hydroclimate reconstruction was performed in the eastern Qinling Mountains, Central China, belonging to the core region of EASM influence. Different from previous studies which are mainly based on total tree-ring width or stable isotope variations, our reconstruction is based on intra-annual tree-ring parameters, namely EWW of *P. tabulaeformis*. The EWW exhibited a much stronger response to MJJ scPDSI than TRW and LWW, indicating that the radial growth of *P. tabulaeformis* is strongly limited by the moisture availability during its early growing season. This highlights the potential of EWW for hydroclimate reconstructions in this area, and possibly beyond in other subtropical regions with similar seasonal patterns of moisture supply. The reconstructed MJJ scPDSI was in-phase with EASMI on decadal and longer timescales before the mid-1950s. Then, the in-phase relationship was replaced by an out-of-phase relationship after the mid-1950s, which might be associated with the intensified dipole pattern of EASM precipitation. Considering the changing spatial characteristics of EASM rainfall, a wider network of intra-annually resolved hydroclimate reconstructions within the core region of EASM influence is necessary to fully capture past EASM changes.

Data availability

The tree-ring data used in this study are available on request (shijf@nju.edu.cn). DWI, precipitation reconstruction, and dry/wet events recorded in historical documents are available from corresponding authors or publications. MADA is available from

https://www.ncdc.noaa.gov/paleo-search/study/10435. The 200 hPa zonal wind dataset of NOAA-20c and JRA-55 are available from https://www.esrl.noaa.gov/psd/data/gridded/data.20thC_ReanV2c.html and https://rda.ucar.edu/datasets/ds628.1/. scPDSI dataset for global land, temperature data of CRU TS 4.01, and precipitation data of GPCC v7 are available from http://climexp.knmi.nl/selectfield_obs2.cgi.

Author contributions

YZ and JS designed the study. JS provided the tree-ring samples. YZ performed tree-ring width measurement, data analyses and interpretation. JS, SS, XS and HL assisted in data interpretation. YZ wrote the first draft of the paper. All authors reviewed the paper.

Competing interests

The authors declare that they have no conflict of interest.

Acknowledgments

The study was supported by the Key R&D Program of China (Grant No. 2016YFA0600503), the National Natural Science Foundation of China (Grant No. 41671193), and the China Scholarship Council (Grant No. 201706190150 and 201806195033). We thank Dr. Feng Chen for providing his reconstructed precipitation data, and Mr. Yu Zhou for his help in tree-ring width measurements.

References

Cai, Q., and Liu, Y.: Climatic response of Chinese pine and PDSI variability in the middle Taihang Mountains, north China since 1873, Trees, 27, 419–427, https://doi.org/10.1007/s00468-012-0812-6, 2012.

Cai, Q., Liu, Y., Lei, Y., Bao, G., and Sun, B.: Reconstruction of the March-August PDSI since 1703 AD based on tree rings of Chinese pine (*Pinus tabulaeformis* Carr.) in the Lingkong Mountain, southeast Chinese Loess Plateau, Clim. Past, 10, 509–521, https://doi.org/10.5194/cp-10-509-2014, 2014.

Cai, Q., Liu, Y., Liu, H., and Ren, J.: Reconstruction of drought variability in North China and its association with sea surface temperature in the joining area of Asia and Indian–Pacific Ocean, Palaeogeogr. Palaeoclimatol. Palaeoecol., 417, 554–560, https://doi.org/10.1016/j.palaeo.2014.10.021, 2015.

Cai, Q., and Liu, Y.: Two centuries temperature variations over subtropical southeast China inferred from *Pinus taiwanensis* Hayata tree-ring width, Clim. Dynam., 1813–1825, https://doi.org/10.1007/s00382-016-3174-8, 2016.

Cai, Q., Liu, Y., Liu, H., Sun, C., and Wang, Y.: Growing-season precipitation since 1872 in the coastal area of subtropical southeast China reconstructed from tree rings and its relationship with the East Asian summer monsoon system, Ecol. Indic., 82, 441–450, https://doi.org/10.1016/j.ecolind.2017.07.012, 2017.

Cai, Q., Liu, Y., Duan, B., Li, Q., Sun, C., and Wang, L.: Tree-ring $\delta^{18}O$, a tool to crack the paleo-hydroclimatic code in subtropical China, Quatern. Int., 487, 3–11, https://doi.org/10.1016/j.quaint.2017.10.038, 2018.

Chen, F., Yuan, Y., Wei, W., Yu, S., Fan, Z., Zhang, R., Zhang, T., and Shang, H.: Tree-ring-based reconstruction of precipitation in the Changling Mountains, China, since A.D.1691, Int. J. Biometeorol., 56, 765–774, https://doi.org/10.1007/s00484-011-0431-8, 2012.

Chen, F., Yuan, Y., Wei, W., Fan, Z., Yu, S., Zhang, T., Zhang, R., Shang, H., and Qin, L.: Reconstructed precipitation for the north-central China over the past 380 years and its linkages to East Asian summer monsoon variability, Quatern. Int., 283, 36–45, https://doi.org/10.1016/j.quaint.2012.05.047, 2013.

Chen, F., Yuan, Y., Zhang, R., and Qin, L.: A tree-ring based drought reconstruction (AD 1760–2010) for the Loess Plateau and its possible driving mechanisms, Global Planet. Change, 122, 82–88, https://doi.org/10.1016/j.gloplacha.2014.08.008, 2014.

Chen, F., Yu, S., Yuan, Y., Wang, H., and Gagen, M.: A tree-ring width based drought reconstruction for southeastern China: links to Pacific Ocean climate variability, Boreas, 45, 335–346, https://doi.org/10.1111/bor.12158, 2016a.

Chen, F., Zhang, R., Wang, H., Qin, L., and Yuan, Y.: Updated precipitation reconstruction (AD 1482–2012) for Huashan, north-central China, Theor. Appl. Climatol., 123, 723–732, https://doi.org/10.1007/s00704-015-1387-0, 2016b.

Compo, G. P., Whitaker, J. S., Sardeshmukh, P. D., Matsui, N., Allan, R. J., Yin, X., Gleason, B. E., Vose, R. S., Rutledge, G., Bessemoulin, P., Brönnimann, S., Brunet, M., Crouthamel, R. I., Grant, A. N., Groisman, P. Y., Jones, P. D., Kruk, M. C., Kruger, A. C., Marshall, G. J., Maugeri, M., Mok, H. Y., Nordli, Ø., Ross, T. F., Trigo, R. M., Wang, X. L., Woodruff, S. D., and Worley, S. J.: The Twentieth Century Reanalysis Project, Quarterly J. Roy. Meteorol. Soc., 137, 1–28, https://doi.org/10.1002/qj.776, 2011.

Cook, E. R.: A time series analysis approach to tree-ring standardization, Ph.D., University of Arizona, Tucson, America, 171 pp., 1985.

Cook, E. R., Meko, D. M., Stahle, D. W., and Cleaveland, M. K.: Drought reconstructions for the continental United States, J. Climate, 12, 1145–1162, 1999.

Cook, E. R., Anchukaitis, K. J., Buckley, B. M., D'Arrigo, R. D., Jacoby, G. C., and Wright, W. E.: Asian monsoon failure and megadrought during the last millennium, Science, 328, 486–489, https://doi.org/10.1126/science.1185188, 2010.

Ding, Y.: Summer monsoon rainfalls in China, J. Meteor. Soc. Japan, 70, 373–396, https://doi.org/10.2151/jmsj1965.70.1B_373, 1992.

Ding, Y., and Dai, X.: Temperature variation in China during the last 100 years, Meteorological Monthly, 20, 19–26, 1994 (in Chinese).

Ding, Y., Wang, Z., and Sun, Y.: Inter-decadal variation of the summer precipitation in East China and its association with decreasing Asian summer monsoon. Part I: Observed evidences, Int. J. Climatol., 28, 1139–1161, https://doi.org/10.1002/joc.1615, 2008.

Ding, Y., Sun, Y., Liu, Y., Si, D., Wang, Z., Zhu, Y., Liu, Y., Song, Y., and Zhang, J.: Interdecadal and interannual variabilities of the Asian summer monsoon and its projection of future change, Chinese J. Atmos. Sci., 37, 253–280, https://doi.org/10.3878/j.issn.1006-9895.2012.12302, 2013 (in Chinese).

Duan, J., Zhang, Q. B., Lv, L., and Zhang, C.: Regional-scale winter-spring temperature variability and chilling damage dynamics over the past two centuries in southeastern China, Clim. Dynam., 39, 919–928, https://doi.org/10.1007/s00382-011-1232-9, 2012.

Fang, K., Gou, X., Chen, F., D'Arrigo, R., and Li, J.: Tree-ring based drought reconstruction for the Guiqing Mountain (China): linkages to the Indian and Pacific Oceans, Int. J. Climatol., 30, 1137–1145, https://doi.org/10.1002/joc.1974, 2009.

Fang, K., Gou, X., Chen, F., Frank, D., Liu, C., Li, J., and Kazmer, M.: Precipitation variability during the past 400 years in the Xiaolong Mountain (central China) inferred from tree rings, Clim. Dynam., 39, 1697–1707, https://doi.org/10.1007/s00382-012-1371-7, 2012a.

Fang, K., Gou, X., Chen, F., Liu, C., Davi, N., Li, J., Zhao, Z., and Li, Y.: Tree-ring based reconstruction of drought variability (1615–2009) in the Kongtong Mountain area, northern China, Global Planet. Change, 80–81, 190–197, https://doi.org/10.1016/j.gloplacha.2011.10.009, 2012b.

Fritts, H. C.: Tree rings and climate, Academic Press, New York, 567 pp., 1976.

Guo, Q., Cai, J., Shao, X., and Sha, W.: Studies on the variations of East-Asian Summer Monsoon during AD 1873~2000, Chinese J. Atmos. Sci., 28, 206–215, 2004 (in Chinese).

Harris, I., Jones, P. D., Osborn, T. J., and Lister, D. H.: Updated high-resolution grids of monthly climatic observations – the CRU TS3.10 dataset. Int. J. Climatol., 34, 623–642, https://doi: 10.1002/joc.3711, 2014.

He, H. W.: The great North-China drought famine of the early Guangxu reign (1876–1879), The Chinese University Press, Hong Kong, 1980 (in Chinese).

Huang, R.-H., Cai, R.-S., Chen, J.-L., and Zhou, L.-T.: Interdecaldal Variations of drought and flooding disasters in China and their association with the East Asian climate system, Chinese J. Atmos. Sci., 30, 730–743, 2006 (in Chinese).

Hughes, M. K., Wu, X. D., Shao, X. M., and Garfin, G. M.: A preliminary reconstruction of rainfall in North-Central China since A.D. 1600 from tree-ring density and width, Quaternary Res., 42, 88–99, https://doi.org/10.1006/qres.1994.1056, 1994.

Jones, P., and Hulme, M.: Calculating regional climatic time series for temperature and precipitation: methods and illustrations, Int. J. Climatol., 16, 361-377, https://doi.org/10.1002/(SICI)1097-0088(199604)16:4<361::AID-JOC53>3.0.CO;2-F, 1996.

Kang, S., Yang, B., Qin, C., Wang, J., Shi, F., and Liu, J.: Extreme drought events in the years 1877–1878, and 1928, in the southeast Qilian Mountains and the air–sea coupling system, Quatern. Int., 283, 85–92, https://doi.org/10.1016/j.quaint.2012.03.011, 2013.

Knapp, P. A., Maxwell, J. T., and Soulé, P. T.: Tropical cyclone rainfall variability in coastal North Carolina derived from longleaf pine (*Pinus palustris* Mill.): AD 1771–2014, Climatic Change, 135, 311–323, https://doi.org/10.1007/s10584-015-1560-6, 2016.

Kobayashi, S., Ota, Y., Harada, Y., Ebita, A., Moriya, M., Onoda, H., Onogi, K., Kamahori, H., Kobayashi, C., Endo, H., Miyaoka, K., and Takahashi, K.: The JRA-55 Reanalysis: general specifications and basic characteristics, J. Met. Soc. Jap., 93, 5–48, https://doi.org/10.2151/jmsj.2015-001, 2015.

Li, J., Chen, F., Cook, E. R., Gou, X., and Zhang, Y.: Drought reconstruction for North Central China from tree rings: the value of the Palmer drought severity index, Int. J. Climatol., 27, 903–909, https://doi.org/10.1002/joc.1450, 2007.

Li, J., Cook, E. R., D'arrigo, R., Chen, F., and Gou, X.: Moisture variability across China and Mongolia: 1951–2005, Clim. Dynam., 32, 1173–1186, https://doi.org/10.1007/s00382-008-0436-0, 2009.

Li, Q., Liu, Y., Song, H., Yang, Y., and Zhao, B.: Divergence of tree-ring-based drought reconstruction between the individual sampling site and the Monsoon Asia Drought Atlas: an example from Guancen Mountain, Sci. Bull., 60, 1688–1697, https://doi.org/10.1007/s11434-015-0889-6, 2015.

Liang, E., and Eckstein, D.: Light rings in Chinese pine (*Pinus tabulaeformis*) in semiarid areas of north China and their palaeo-climatological potential, New Phytol., 171, 783–791, https://doi.org/10.1111/j.1469-8137.2006.01775.x, 2006.

Liang, E., Liu, X., Yuan, Y., Qin, N., Fang, X., Huang, L., Zhu, H., Wang, L., and Shao, X.: The 1920s drought recorded by tree rings and historical documents in the semi-arid and arid areas of Northern China, Climatic Change, 79, 403–432, https://doi.org/10.1007/s10584-006-9082-x, 2006.

Liang, E., Shao, X., Liu, H., and Eckstein, D.: Tree-ring based PDSI reconstruction since AD 1842 in the Ortindag Sand Land, east Inner Mongolia, Chinese Sci. Bull., 52, 2715–2721, https://doi.org/10.1007/s11434-007-0351-5, 2007.

Liang, E., Eckstein, D., and Shao, X.: Seasonal cambial activity of relict Chinese Pine at the northern limit of its natural distribution in North China - exploratory results, IAWA J., 30, 371–378, 2009.

Liu, H., Shao, X., and Huang, L.: Reconstruction of early-summer drought indices in mid-north region of China after 1500 using tree ring chronologies, Quaternary Sciences, 22, 220–229, 2002 (in Chinese).

Liu, Y., Liu, H., Song, H., Li, Q., Burr, G. S., Wang, L., and Hu, S.: A monsoon-related 174-year relative humidity record from tree-ring $\delta^{18}O$ in the Yaoshan region, eastern central China, Sci. Total. Environ., 593–594, 523–534, https://doi.org/10.1016/j.scitotenv.2017.03.198, 2017a.

Liu, Y., Zhang, X., Song, H., Cai, Q., Li, Q., Zhao, B., Liu, H., and Mei, R.: Tree-ring-width-based PDSI reconstruction for central Inner Mongolia, China over the past 333 years, Clim. Dynam., 48, 867–879, https://doi.org/10.1007/s00382-016-3115-6, 2017b.

Meko, D., and Graybill, D. A.: Tree-ring reconstruction of upper Gila River discharge, Water Resour. Bull., 31, 605–616, https://doi.org/10.1111/j.1752-1688.1995.tb03388.x, 1995.

Osborn, T. J., Briffa, K. R., and Jones, P. D.: Adjusting variance for sample-size in tree ring chronologies and other regional-mean time-series, Dendrochronologia, 15, 89–99, 1997.

Palmer, W. C., Meteorological drought, U.S. Department of Commerce, Weather Bureau Research Paper 45, 58 pp., 1965.

Pei, L., Yan, Z., and Yang, H.: Multidecadal variability of dry/wet patterns in eastern China and their relationship with the Pacific Decadal Oscillation in the last 413 years, Chinese Sci. Bull., 60, 97–108, https://doi.org/10.1360/n972014-00790, 2015 (in Chinese).

Schneider, U., Becker, A., Finger, P., Meyer-Christoffer, A., Rudolf, B., and Ziese, M.: GPCC full data monthly product version 7.0 at 0.5°: Monthly land-surface precipitation from rain-gauges built on GTS-based and historic data, https://doi.org/10.5676/DWD_GPCC/FD_M_V7_050, 2015.

Shi, J.F., Liu, Y., Vaganov, E. V., Li, J. B., Cai, Q. F.: Statistical and process-based modeling anlyses of tree growth response to climate in semi-arid area of north central China: A case study of *Pinus tabulaeformis*, J. Geophys. Res., 113, G01026, https://doi.org/10.1029/2007JG000547, 2008

Shi, J. F., Cook, E. R., Lu, H. Y., Li, J. B., Wright, W. E., and Li, S. F.: Tree-ring based winter temperature reconstruction for the lower reaches of the Yangtze River in southeast China, Clim. Res., 41, 169–175, https://doi.org/10.3354/cr00851, 2010.

Shi, J., Li, J., Cook, E. R., Zhang, X., and Lu, H.: Growth response of *Pinus tabulaeformis* to climate along an elevation gradient in the eastern Qinling Mountains, central China, Clim. Res., 53, 157–167, https://doi.org/10.3354/cr01098, 2012.

Shi, J., Lu, H., Li, J., Shi, S., Hou, X., and Li, L.: Tree-ring based February–April precipitation reconstruction for the lower reaches of the Yangtze River, Southeast China, Global Planet. Change, 131, 82–88, https://doi.org/10.1016/j.gloplacha.2015.05.006, 2015.

Shi, J., Li, J., Zhang, D. D., Zheng, J., Shi, S., Ge, Q., Lee, H. F., Zhao, Y., Zhang, J., and Lu, H.: Two centuries of April-July temperature change in southeastern China and its influence on grain productivity, Sci. Bull., 62, 40–45, https://doi.org/10.1016/j.scib.2016.11.005, 2017.

Si, D., and Ding, Y.: Oceanic forcings of the interdecadal variability in East Asian summer rainfall, J. Climate, 29, 7633–7649, https://doi.org/10.1175/jcli-d-15-0792.1, 2016.

Song, H., and Liu, Y.: PDSI variations at Kongtong Mountain, China, inferred from a 283-year *Pinus tabulaeformis* ring width chronology, J. Geophys. Res.-Atmos., 116, https://doi.org/10.1029/2011jd016220, 2011.

Stahle, D. W., Cleaveland, M. K., Fye, F. K., Burnette, D. J., Grissino-Mayer, H. D., Therrell, M. D., Griffin, R. D., Meko, D. M., and Villanueva Diaz, J.: Cool- and warm-season precipitation reconstructions over western New Mexico, J. Climate, 22, 3729–3750, https://doi.org/10.1175/2008JCLI2752.1, 2009.

Sun, J., Liu, Y., Sun, B., and Wang, R.: Tree-ring based PDSI reconstruction since 1853 AD in the source of the Fenhe river basin, Shanxi province, China, Sci. China Earth Sci., 55, 1847–1854, https://doi.org/10.1007/s11430-012-4369-4, 2012.

van der Schrier, G., Barichivich, J., Briffa, K. R., and Jones, P. D.: A scPDSI-based global data set of dry and wet spells for 1901-2009, J. Geophys. Res.-Atmos., 118, 4025–4048, https://doi.org/10.1002/jgrd.50355, 2013.

Wang, B., Wu, Z., Li, J., Liu, J., Chang, C.-P., Ding, Y., and Wu, G.: How to measure the strength of the East Asian Summer Monsoon, J. Climate, 21, 4449–4463, https://doi.org/10.1175/2008jcli2183.1, 2008.

Wang, D., and Wang, A.: Applicability assessment of GPCC and CRU precipitation products in China during 1901 to 2013, Climatic and Environmental Research, 22, 446–462, https://doi.org/10.3878/j.issn.1006-9585.2016.16122, 2017 (in Chinese).

Wang, S., Gong, D., Ye, J., and Chen, Z.: Seasonal precipitation series of Eastern China since 1880 and the variability, Acta Geographic Sinica, 55, 281–293, 2000 (in Chinese).

Wang, Z., Li, J., Lai, C., Zeng, Z., Zhong, R., Chen, X., Zhou, X., and Wang, M.: Does drought in China show a significant decreasing trend from 1961 to 2009?, Sci. Total. Environ., 579, 314–324, https://doi.org/10.1016/j.scitotenv.2016.11.098, 2017.

Wen, K.: Meteorological disasters in China, China Meteorological Press, Beijing, China, 2006 (in Chinese).

Wen, X.-Y., Wang, S.-W., Zhu, J.-H., and David, V.: An overview of China climate change over the 20th century using UK/UEA/CRU high resolution grid data, Chinese J. Atmos. Sci., 30, 894–903, 2006 (in Chinese).

Wigley, T. M. L., Briffa, K. R., and Jones, P. D.: On the average value of correlated time series, with applications in dendroclimatology and hydrometeorology, J. Clim. App. Meteorol., 23, 201–213, https://doi.org/10.1175/1520-0450(1984)023<0201:otavoc>2.0.co;2, 1984.

Xu, C., Ge, J., Nakatsuka, T., Yi, L., Zheng, H., and Sano, M.: Potential utility of tree ring $\delta^{18}O$ series for reconstructing precipitation records from the lower reaches of the Yangtze River, southeast China, J. Geophys. Res. Atmos., 121, 3954–3968, https://doi.org/10.1002/2015JD023610, 2016.

Xu, C., Shi, J., Zhao, Y., Nakatsuka, T., Sano, M., Shi, S., and Guo, Z.: Early summer precipitation in the lower Yangtze River basin for AD 1845–2011 based on tree-ring cellulose oxygen isotopes, Clim. Dynam., https://doi.org/10.1007/s00382-018-4212-5, 2018.

Yang, B., Kang, S., Ljungqvist, F. C., He, M., Zhao, Y., and Qin, C.: Drought variability at the northern fringe of the Asian summer monsoon region over the past millennia, Clim. Dynam., 43, 845–859, https://doi.org/10.1007/s00382-013-1962-y, 2013a.

Yang, F., Shi, F., Kang, S., Wang, S., Xiao, Z., Nakatsuka, T., and Shi, J.: Comparison of the dryness/wetness index in China with the Monsoon Asia Drought Atlas, Theor. Appl. Climatol., 114, 553–566, https://doi.org/10.1007/s00704-013-0858-4, 2013b.

Yan, H.-M., Zhong, M., and Zhu, Y.-Z.: The determination of degrees of freedom for digital filtered time series——An Application in the correlation analysis between length of day variation and SOI, Acta Astronomica Sinica, 44, 324–329, 2003 (in Chinese).

Zeng, Q., Rossi, S., and Yang, B.: Effects of age and size on xylem phenology in two conifers of Northwestern China, Front. Plant. Sci., 8, 2264, https://doi.org/10.3389/fpls.2017.02264, 2018.

Zhang, Y., Tian, Q., Guillet, S., and Stoffel, M.: 500-yr. precipitation variability in Southern Taihang Mountains, China, and its linkages to ENSO and PDO, Climatic Change, 144, 419–432, https://doi.org/10.1007/s10584-016-1695-0, 2017.

Zhao, G., Huang, G., Wu, R., Tao, W., Gong, H., Qu, X., and Hu, K.: A new upper-level circulation index for the East Asian Summer Monsoon variability, J. Climate, 28, 9977–9996, https://doi.org/10.1175/jcli-d-15-0272.1, 2015.

Zhao, Y., Shi, J., Shi, S., Wang, B., and Yu, J.: Summer climate implications of tree-ring latewood width: a case study of *Tsuga longibracteata* in South China, Asian Geographer, 34, 131–146, https://doi.org/10.1080/10225706.2017.1377623, 2017a.

Zhao, Y., Shi, J., Shi, S., Yu, J., and Lu, H.: Tree-ring latewood width based July–August SPEI reconstruction in South China since 1888 and its possible connection with ENSO, J. Meteorol. Res.-PRC, 31, 39–48, https://doi.org/10.1007/s13351-017-6096-4, 2017b.

Zheng, Y., Zhang, Y., Shao, X., Yin, Z.-Y., and Zhang, J.: Temperature variability inferred from tree-ring widths in the Dabie Mountains of subtropical central China, Trees, 26, 1887–1894, https://doi.org/10.1007/s00468-012-0757-9, 2012.

Zhou, T., Gong, D., Li, J., and Li, B.: Detecting and understanding the multi-decadal variability of the East Asian Summer Monsoon - Recent progress and state of affairs, Meteorologische Zeitschrift, 18, 455–467, https://doi.org/10.1127/0941-2948/2009/0396, 2009.

Zhou, T., Song, F., Ha, K.-J., and Chen, X.: Decadal change of East Asian Summer Monsoon: contributions of internal variability and external forcing, in: The Global Monsoon System: 3rd ed., World Scientific, 327–336, 2017.

Clim. Past Discuss., https://doi.org/10.5194/cp-2018-141
Manuscript under review for journal Clim. Past
Discussion started: 29 October 2018

Climate of the Past Discussions
Open Access
EGU

Table 1. Statistics for split calibration-verification of the regression model.

Calibration period	*R*	R^2	Verification period	*RE*	*CE*	Sign-test
Full period (1951–2005)	0.71**	0.50**	—	—	—	—
Early half (1951–1978)	0.68**	0.46**	Late half (1978–2005)	0.58	0.56	25+/3–**
Late half (1978–2005)	0.75**	0.56**	Early half (1951–1978)	0.47	0.43	23+/5–**

** $p < 0.01$; *r*, Pearson correlation coefficient; R^2, explained variance; *RE*, reduction of error; and *CE*, coefficient of efficiency.

Clim. Past Discuss., https://doi.org/10.5194/cp-2018-141
Manuscript under review for journal Clim. Past
Discussion started: 29 October 2018

Climate of the Past Discussions
Open Access
EGU

Table 2. Moderately to severely dry (scPDSI ⩽ –1.71) and wet (scPDSI ⩾ 2.29) events derived from the MJJ scPDSI reconstruction and corresponding descriptions from historical documents.

Event type	Year	scPDSI	Description
Dry	1874	–1.73	Summer drought at Junxian (Northwest Hubei)
	1879	–3.60	A mega-drought occurred has caused a great famine over Henan, Shaanxi and other provinces in North China in the early Guangxu reign (1876–1879)[a]
	1880	–2.03	Not available
	1900	–2.22	Severe summer drought over Shaanxi
	1902	−1.93	Drought from spring to summer over Henan
	1920	−1.73	Drought from spring to autumn over Henan; No rainfall over Shaanxi since summer
	1923	–2.22	Drought over Henan and Shaanxi
	1926	–2.30	No harvest at Ruyang (West Henan) due to severe drought
	1928	−1.76	Summer drought over Henan, Shaanxi and Northwest Hubei
	1929	–2.47	Summer drought over Henan and Shaanxi
Wet	1883	2.32	Persistent rainfall in summer at Shanxian and Mianchi (Northwest Henan)
	1885	2.76	Flood in summer at Lingbao and Shanxian (Northwest Henan)
	1894	2.76	Not available
	1898	3.60	Severe flood in summer at Lushi (Northwest Henan), Shangnan (Southeast Shaanxi) and Danjiang (Northwest Hubei)
	1906	3.45	Heavy rainfall in summer over Henan
	1911	3.64	Heavy rainfall in summer over Henan

Clim. Past Discuss., https://doi.org/10.5194/cp-2018-141
Manuscript under review for journal Clim. Past
Discussion started: 29 October 2018

	1933	2.45	Heavy rainfall in summer over Henan and Shaanxi
	1934	3.06	Summer rainfall over Henan, South Shaanxi and Northwest Hubei
	1936	3.65	Not available
	1948	2.66	Wheat loss caused by summer rainfall
	1949	2.82	Not available

[a] Historical description of the 1879 drought event is cited from He (1980), and others are cited from Wen (2006)

Clim. Past Discuss., https://doi.org/10.5194/cp-2018-141
Manuscript under review for journal Clim. Past
Discussion started: 29 October 2018

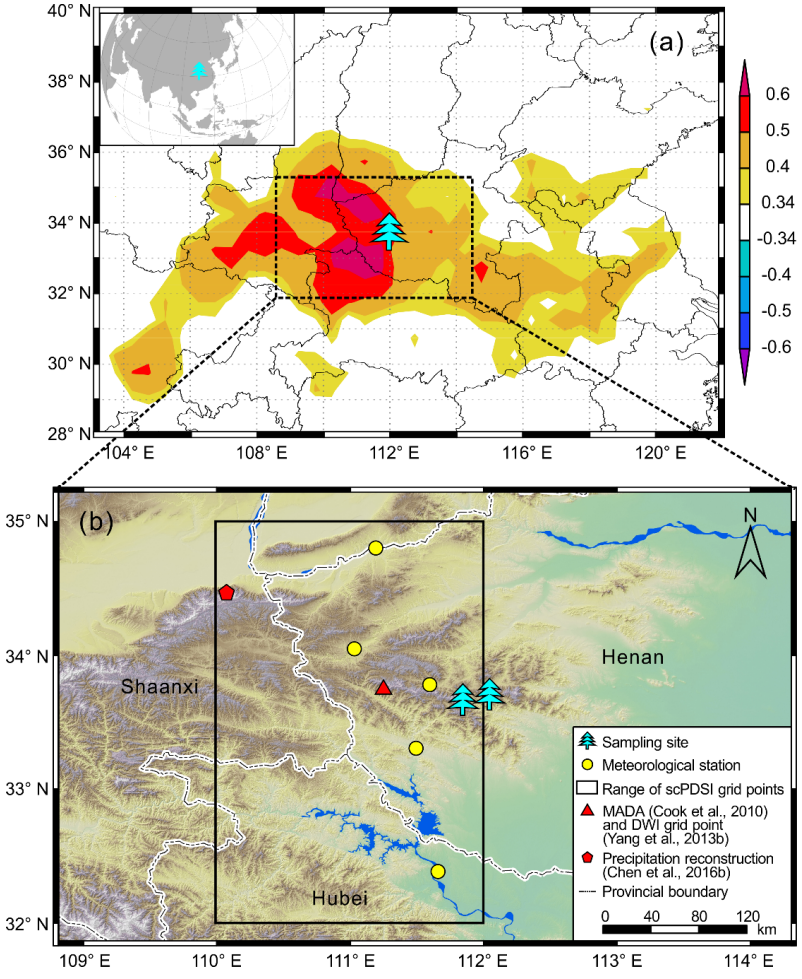

Figure 1. Map of the study region. **(a)** Location of the sampling site (tree symbol), and the spatial correlations between tree-ring earlywood width chronology and May–July (MJJ) scPDSI during the period 1951–2005. **(b)** Locations of the meteorological stations (cycle), Monsoon Asia Drought Atlas (MADA; Cook et al., 2010) and Dryness/Wetness Index (DWI; Yang et al., 2013b) grid point (triangle), and tree-ring width based precipitation reconstruction (pentagon; Chen et al., 2016b), and the range of the averaged scPDSI grid points (rectangle; van der Schrier et al., 2013).

Clim. Past Discuss., https://doi.org/10.5194/cp-2018-141
Manuscript under review for journal Clim. Past
Discussion started: 29 October 2018

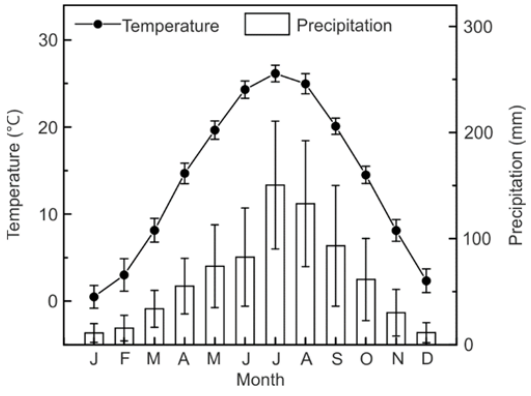

Figure 2. Monthly mean temperature and monthly total precipitation averaged from the five selected meteorological stations during the period 1951–2005. Error bars denotes ± one standard deviations.

Clim. Past Discuss., https://doi.org/10.5194/cp-2018-141
Manuscript under review for journal Clim. Past
Discussion started: 29 October 2018

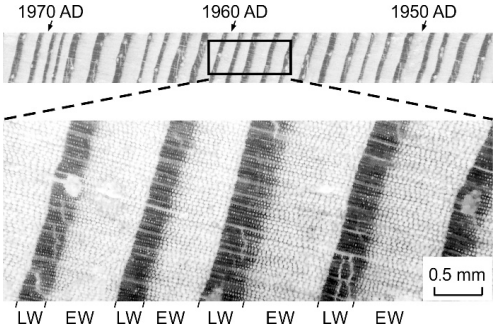

Figure 3. Scanned photograph of a piece of *P. tabulaeformis* tree-ring sample. The distinct earlywood (EW) and latewood (LW) segments can be identified by inspection under a microscope.

Clim. Past Discuss., https://doi.org/10.5194/cp-2018-141
Manuscript under review for journal Clim. Past
Discussion started: 29 October 2018

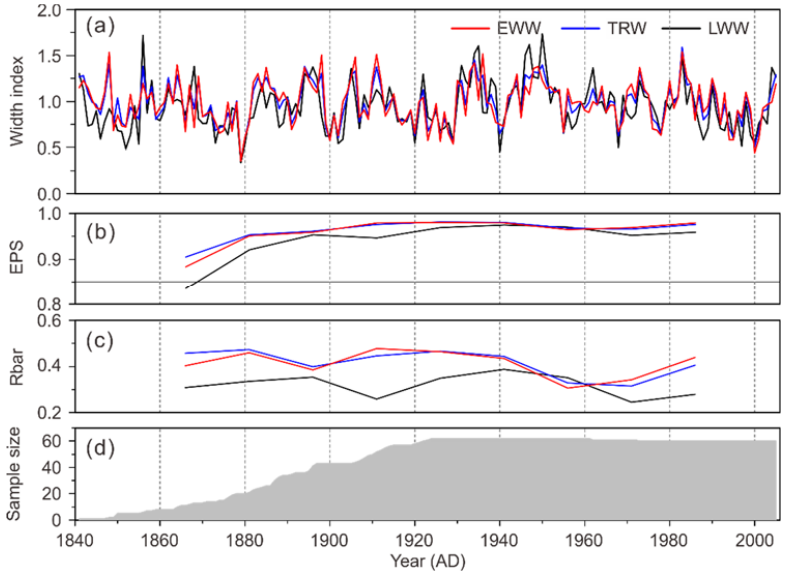

Figure 4. Tree-ring standardized width chronologies and their corresponding statistics. **(a)** Width chronologies of earlywood (EWW, red), total tree-ring width (TRW, blue) and latewood width (LWW, black); **(b)** Running expressed population signal (EPS); **(c)** Running Rbar; **(d)** Sample size. The running EPS and Rbar values were calculated over a 30-year window with a 15-year overlap. The horizontal line in **(b)** indicates the threshold EPS value of 0.85.

Clim. Past Discuss., https://doi.org/10.5194/cp-2018-141
Manuscript under review for journal Clim. Past
Discussion started: 29 October 2018

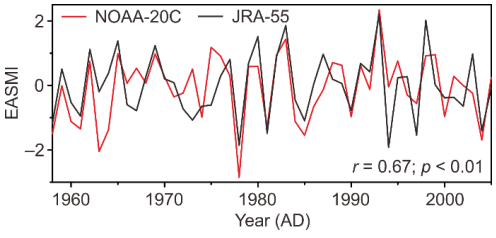

Figure 5. Normalized MJJ EASMI (1958–2005) calculated according to the definition of Zhao et al., (2015) using 200 hPa zonal wind dataset from NOAA-20C (red line) and JRA-55 (black line).

Clim. Past Discuss., https://doi.org/10.5194/cp-2018-141
Manuscript under review for journal Clim. Past
Discussion started: 29 October 2018

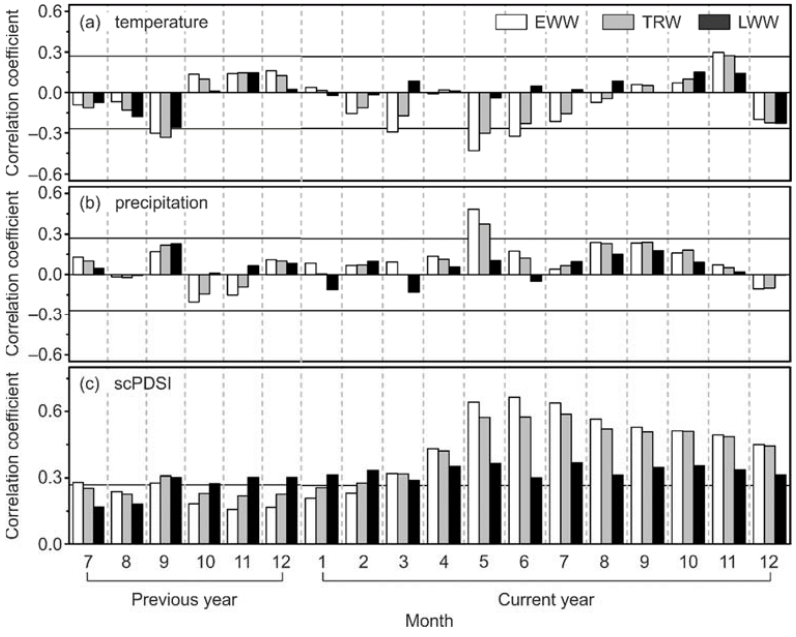

Figure 6. Correlation coefficients between tree-ring width chronologies and climatic factors for EWW (white), TRW (grey) and LWW (black) during their common period 1951–2005. The climatic factors are **(a)** monthly mean temperature, **(b)** monthly total precipitation, and **(c)** monthly scPDSI. Horizontal lines indicate the 0.05 significance level.

Clim. Past Discuss., https://doi.org/10.5194/cp-2018-141
Manuscript under review for journal Clim. Past
Discussion started: 29 October 2018

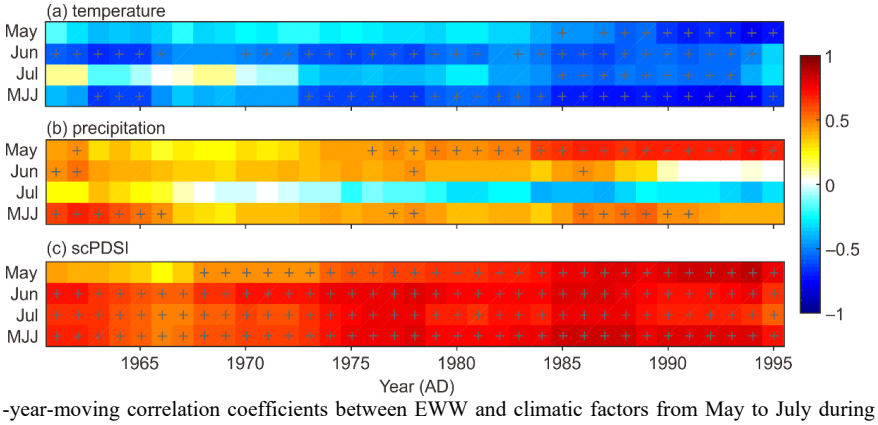

Figure 7. 21-year-moving correlation coefficients between EWW and climatic factors from May to July during the period 1951–2005. The climatic factors are **(a)** monthly mean temperature, **(b)** monthly total precipitation, and **(c)** monthly scPDSI. MJJ denotes May–July. Grids with crosses indicate that the correlation is statistically significant ($p < 0.05$).

Clim. Past Discuss., https://doi.org/10.5194/cp-2018-141
Manuscript under review for journal Clim. Past
Discussion started: 29 October 2018

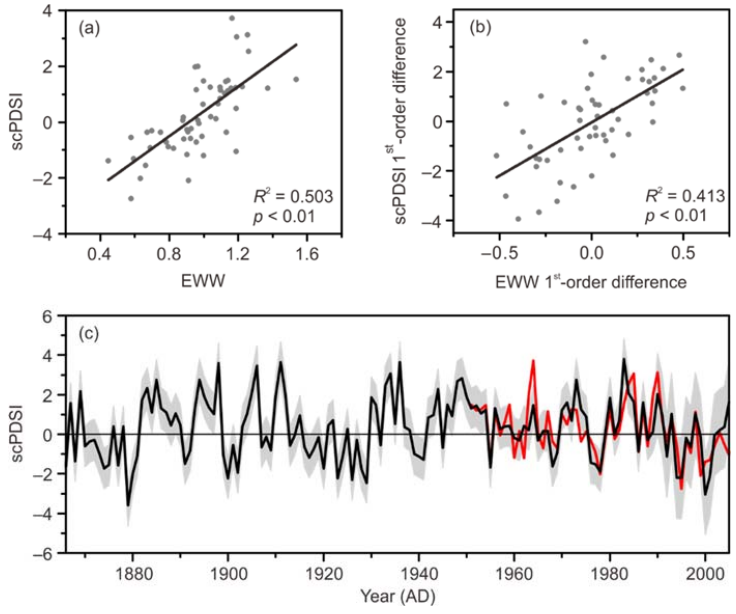

Figure 8. Scatter diagram of EWW chronology versus MJJ scPDSI for their **(a)** raw time series, and **(b)** first-order difference during the period 1951–2005. **(c)** MJJ scPDSI reconstruction (black line) and instrumental MJJ scPDSI (red line). Shade area denotes the uncertainties of reconstruction in the form of ± 1 root mean square error.

Clim. Past Discuss., https://doi.org/10.5194/cp-2018-141
Manuscript under review for journal Clim. Past
Discussion started: 29 October 2018

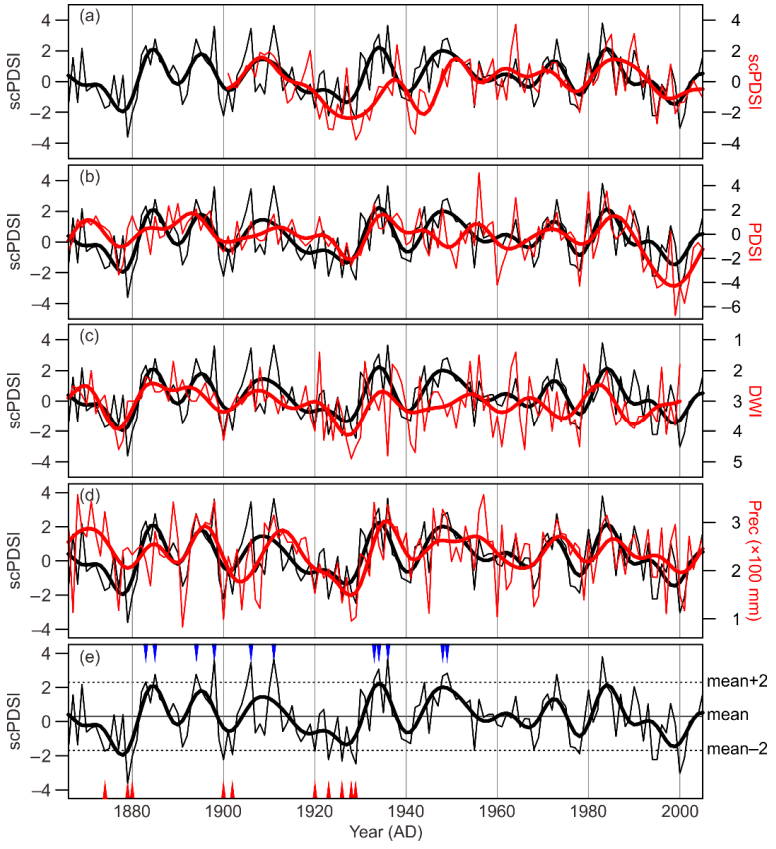

Figure 9. Comparison of **(e)** the reconstructed MJJ scPDSI with **(a)** MJJ scPDSI extracted from the scPDSI database (van der Schrier et al., 2013), **(b)** June–August PDSI of MADA 370 (Cook et al., 2010), **(c)** DWI (Yang et al., 2013), and **(d)** TRW based April–June precipitation (prec) reconstruction (Chen et al., 2016b). Thin line denotes the original series, thick line the 10-year low-pass filtered values. The red and blue triangles are dry and wet events deduced from historical documents.

Clim. Past Discuss., https://doi.org/10.5194/cp-2018-141
Manuscript under review for journal Clim. Past
Discussion started: 29 October 2018

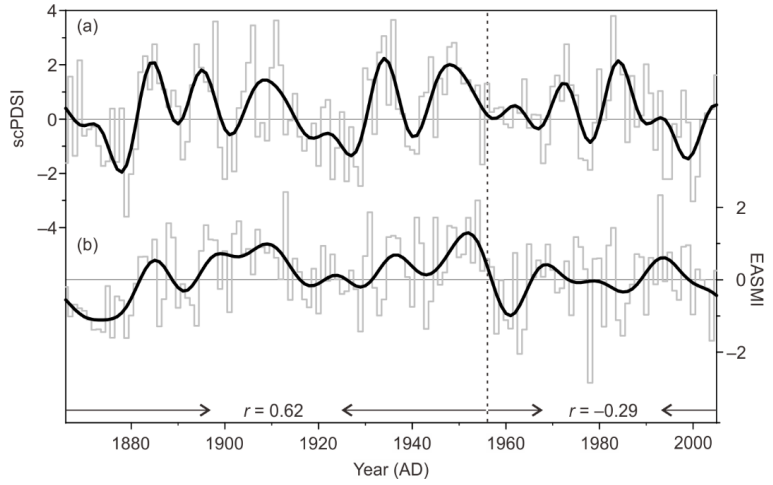

Figure 10. Comparison between the **(a)** MJJ scPDSI reconstruction and **(b)** EASMI. Gray and black lines denote the raw time series and decadal filtered values, respectively. The vertical dashed line denotes the year 1956. *r* means the correlation coefficient between the decadal filtered MJJ scPDSI and EASMI.

Clim. Past Discuss., https://doi.org/10.5194/cp-2018-141
Manuscript under review for journal Clim. Past
Discussion started: 29 October 2018

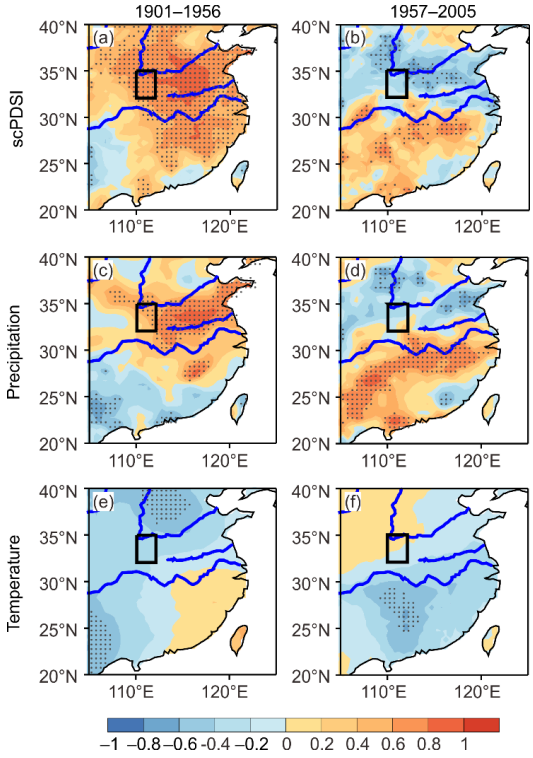

Figure 11. Spatial correlation patterns between the decadal filtered EASMI and **(a–b)** scPDSI, **(c–d)** precipitation, and **(e–f)** temperature in MJJ for the periods 1901-1956 (left panels) and 1957-2005 (right panels). The dot indicates that the correlation is statistically significant ($p < 0.1$). The rectangle denotes the study region for hydroclimate reconstruction. Blue curves from north to south represent the Yellow River, Huaihe River, and Yangtze River, respectively.